Ab-initio study of Si(111) square root 3* square root 3-Sn using molecular dynamics total energy methods

1990 J. Phys.: Condens. Matter 2 7435

(http://iopscience.iop.org/0953-8984/2/36/006)

J. Phys.: Condens. Matter 2 (1990) 7435–7443. Printed in the UK

Ab-initio study of Si(111) $\sqrt{3} \times \sqrt{3}$–Sn using molecular dynamics total energy methods

S K Ramchurn, D M Bird and D W Bullett
School of Physics, University of Bath, Bath BA2 7AY, UK

Abstract. An *ab-initio* relaxation of the Si(111) $\sqrt{3} \times \sqrt{3}$–Sn structure is performed. The LDA total energy is minimized using the molecular dynamics method of Car and Parrinello, with the inclusion of separable, non-local pseudopotentials. The pseudopotential implementation is discussed in detail. Competing sites for the Sn adatom are investigated. Results agree well with recent x-ray diffraction experiments.

1. Introduction

It is now well established that the calculation of total energies within the local density approximation (LDA) can be sufficiently accurate for the equilibrium structures of, for example, crystals, defects and surfaces to be predicted with some confidence. Most work has been carried out on semiconductors and has used a pseudopotential formalism to calculate the total energy (for recent reviews see Srivastava and Weaire 1987 and Ihm 1988). The method is now being applied to increasingly large and complex systems (e.g. adsorbates on surfaces) where experimental determination of the structure is often very difficult and where theoretical prediction of the relaxed structure and comparison between competing adsorbate sites can provide considerable insight into the adsorbate–substrate interaction (e.g. Meade and Vanderbilt 1989, Bedrossian *et al* 1989, Lyo *et al* 1989). Allied to the increase in the size of the systems studied is a dramatic increase in the computational time required, and considerable effort has been made to increase the efficiency of the calculations. The most significant of these improvements is the introduction of some kind of iterative diagonalization technique (e.g. Meade and Vanderbilt 1989, Nex 1987) where the number of operations required for diagonalization of an $N \times N$ matrix scales with N considerably slower than the standard N^3. In a pseudopotential calculation N will be the number of plane waves that are required at each $\boldsymbol{k}$-point to give a good description of the valence wavefunctions. With an N^3 dependence it rapidly becomes prohibitive to perform calculations on structures with a large unit cell or where (for example, in oxides or transition metal compounds) pseudopotentials are relatively strong and a large number of plane waves are required to provide accurate wavefunctions.

One of the most attractive of the iterative methods is that introduced by Car and Parrinello (1985) which combines molecular dynamics techniques with a pseudopotential total energy formalism to relax both the electrons and ions to their ground state configurations. A particular feature of this approach is that the electrons and ions are treated on the same footing, so that it is not necessary to generate fully self-consistent electronic configurations every time the forces on the ions are calculated. Instead, the ions are moved in response to the forces calculated at each molecular dynamics

0953-8984/90/367435+09$03.50

timestep, and as energy is removed from the system (by damping) the electrons and ions settle into an equilibrium structure. Provided the ionic displacements at each step are small the ions and electrons remain in approximate equilibrium throughout the molecular dynamics calculation, and by judicious choice of the timestep and damping factors convergence to the ground state can be fairly swift (Payne *et al* 1986). Although it is not guaranteed that in any one run the true ground state is found, by performing runs with different starting configurations the danger of finding metastable solutions can be reduced. The molecular dynamics method has been extended by Payne *et al* (1986), and by Allan and Teter (1987) and has been successfully applied to a number of systems (Ballone *et al* 1988, Payne *et al* 1987, Needels *et al* 1987, Payne 1987, for a recent review see Payne *et al* 1990). One technical problem in using the molecular dynamics method is that non-local pseudopotentials are rather difficult to handle—much of the work in the above papers refers to Ge which is rather well described by a *local* pseudopotential. In the general case it is important to be able to handle non-local potentials; the details of why these potentials cause a problem, the way in which we have included them and the results of test calculations are described in section 2. In section 3 we apply the molecular dynamics method to the Si(111) $\sqrt{3} \times \sqrt{3}$–Sn structure in order to compare our predicted structure with that recently determined by grazing-angle x-ray studies (Conway *et al* 1989).

2. The molecular dynamics method

In a pseudopotential total energy calculation the valence wavefunctions Ψ_n are expanded using a plane-wave basis set

$$\Psi_n(\boldsymbol{r}) = \sum_{\boldsymbol{g}} c_{n,\boldsymbol{g}}(\boldsymbol{k}) \exp[\mathrm{i}(\boldsymbol{k}+\boldsymbol{g})\cdot\boldsymbol{r}] \tag{1}$$

where the $c_{n,\boldsymbol{g}}(\boldsymbol{k})$ are the plane wave coefficients for state n at $\boldsymbol{k}$-point $\boldsymbol{k}$. The Car–Parrinello equations of motion for these coefficients become (Payne *et al* 1986)

$$\mu\ddot{c}_{n,\boldsymbol{g}}(\boldsymbol{k}) = \left[-\frac{\hbar^2}{2m}(\boldsymbol{k}+\boldsymbol{g})^2 + \lambda_{n,\boldsymbol{k}}\right] c_{n,\boldsymbol{g}}(\boldsymbol{k}) - \sum_{\boldsymbol{g}'}\left[V_{\mathrm{H}}(\boldsymbol{g}-\boldsymbol{g}') + V_{\mathrm{xc}}(\boldsymbol{g}-\boldsymbol{g}') + V_{\mathrm{ion}}(\boldsymbol{k}+\boldsymbol{g},\boldsymbol{k}+\boldsymbol{g}')\right] c_{n,\boldsymbol{g}'}(\boldsymbol{k}) \tag{2}$$

where μ is the fictitious mass given to the coefficients, the λ_n are the expectation values of the Kohn–Sham Hamiltonian (Kohn and Sham 1965) for state n (which in equilibrium become the Kohn–Sham eigenvalues), and V_{H}, V_{xc} and V_{ion} are the Hartree, exchange correlation and ionic pseudopotential parts respectively of the Kohn–Sham potential. With a local pseudopotential, the V_{ion} term also becomes simply a function of $(\boldsymbol{g}-\boldsymbol{g}')$ and by using fast Fourier transforms (FFTs) between real and reciprocal space the 'force' terms on the right-hand side of (2) can be calculated for *all* $\boldsymbol{g}$ in $\sim N \ln N$ operations. Note that N here refers to the number of grid points (in both real and reciprocal space) used in the three-dimensional FFTs and is greater, typically by a factor of about three, than the number of plane waves $\boldsymbol{g}$ for which the coefficients are calculated in (1) and (2). This is because the grid points must form a regular 'box', while the included vectors $\boldsymbol{g}$ are usually chosen to lie within a sphere of a given cut-off

radius. The reduction in the number of operations which the FFTs allow is vital to the success of the molecular dynamics method because, in principle, it allows calculations with very large basis sets to be performed. The problem with non-local potentials is now apparent: in (2) it would seem that for each of the N $\boldsymbol{g}$ on the left hand side we must sum over N $\boldsymbol{g}'$ on the right, a total of N^2 operations. Combined with the relatively large number of timesteps which are needed for convergence of the molecular dynamics, this N^2 dependence would remove any advantage the Car–Parrinello scheme has over conventional diagonalization.

It is therefore essential to reduce the N^2 scaling. This has been achieved by Allan and Teter (1987) by using the *separable* pseudopotentials introduced by Kleinman and Bylander (1982). Here, a local part of the potential, V^{L} is separated out:

$$V_{\mathrm{ion}}(\boldsymbol{k}+\boldsymbol{g},\boldsymbol{k}+\boldsymbol{g}') = V^{\mathrm{L}}(\boldsymbol{g}-\boldsymbol{g}') + V^{\mathrm{NL}}(\boldsymbol{k}+\boldsymbol{g},\boldsymbol{k}+\boldsymbol{g}') \tag{3}$$

and, for a single atomic species, the non-local contribution, V^{NL}, is written

$$V^{\mathrm{NL}}(\boldsymbol{q},\boldsymbol{q}') = \sum_l 4\pi(2l+1)P_l(\cos\theta_{\boldsymbol{q}\boldsymbol{q}'})\frac{I_l(q)\,I_l(q')}{I_l^{\mathrm{s}}} \tag{4}$$

where P_l is the Legendre polynomial of order l and $\theta_{\boldsymbol{q}\boldsymbol{q}'}$ is the angle between $\boldsymbol{q}$ and $\boldsymbol{q}'$. $I_l(q)$ and I_l^{s} are projection and scaling integrals, respectively:

$$I_l(q) = \int_0^\infty \mathrm{d}r\, r^2 j_l(qr)\phi_l(r)\Delta V_l(r) \tag{5a}$$

$$I_l^{\mathrm{s}} = \int_0^\infty \mathrm{d}r\, r^2[\phi_l(r)]^2\Delta V_l(r). \tag{5b}$$

where j_l is a spherical Bessel function of order l, $\phi_l(r)$ is the radial part of the pseudo-wavefunction used to generate the pseudopotential component $V_l(r)$ and ΔV_l is the difference between this and the local potential $V^{\mathrm{L}}(r)$:

$$\Delta V_l(r) = V_l(r) - V^{\mathrm{L}}(r). \tag{6}$$

As usual, we include only the $l = 0, 1$ and 2 components, in which case the non-local contribution to the 'force' in (2) can be written:

$$\frac{4\pi}{\Omega I_{\mu,0}^{\mathrm{s}}}\sum_\mu\left(\exp(-\mathrm{i}\boldsymbol{g}\cdot\boldsymbol{r}_\mu)\,I_{\mu,0}(k+g)\sum_{\boldsymbol{g}'}c_{n,\boldsymbol{g}'}\exp(\mathrm{i}\boldsymbol{g}'\cdot\boldsymbol{r}_\mu)\,I_{\mu,0}(k+g')\right) \tag{7a}$$

$$+\frac{12\pi}{\Omega I_{\mu,1}^{\mathrm{s}}}\sum_{\mu,i}\left(\frac{(\boldsymbol{k}+\boldsymbol{g})_i}{k+g}\exp(-\mathrm{i}\boldsymbol{g}\cdot\boldsymbol{r}_\mu)\,I_{\mu,1}(k+g)\right.$$

$$\left.\times\sum_{\boldsymbol{g}'}c_{n,\boldsymbol{g}'}\frac{(\boldsymbol{k}+\boldsymbol{g}')_i}{k+g'}\exp(\mathrm{i}\boldsymbol{g}'\cdot\boldsymbol{r}_\mu)\,I_{\mu,1}(k+g')\right) \tag{7b}$$

$$-\frac{10\pi}{\Omega I_{\mu,2}^{\mathrm{s}}}\sum_\mu\left(\exp(-\mathrm{i}\boldsymbol{g}\cdot\boldsymbol{r}_\mu)\,I_{\mu,2}(k+g)\sum_{\boldsymbol{g}'}c_{n,\boldsymbol{g}'}\exp(\mathrm{i}\boldsymbol{g}'\cdot\boldsymbol{r}_\mu)\,I_{\mu,2}(k+g')\right)$$

$$+\frac{30\pi}{\Omega I_{\mu,2}^{\mathrm{s}}}\sum_{\mu,i,j}\left(\frac{(\boldsymbol{k}+\boldsymbol{g})_i(\boldsymbol{k}+\boldsymbol{g})_j}{(k+g)^2}\exp(-\mathrm{i}\boldsymbol{g}\cdot\boldsymbol{r}_\mu)\,I_{\mu,2}(k+g)\right.$$

$$\left.\times\sum_{\boldsymbol{g}'}c_{n,\boldsymbol{g}'}\frac{(\boldsymbol{k}+\boldsymbol{g}')_i(\boldsymbol{k}+\boldsymbol{g}')_j}{(k+g')^2}\exp(\mathrm{i}\boldsymbol{g}'\cdot\boldsymbol{r}_\mu)\,I_{\mu,2}(k+g')\right). \tag{7c}$$

(7*a*), (7*b*) and (7*c*) represent the s, p and d contributions respectively. In these equations we have explicitly included the structure dependent terms which depend on the atomic coordinates $\boldsymbol{r}_\mu$. To indicate that there may be more than one species of atom in the unit cell the projection and scaling integrals also have a label μ. The sums over i and j represent sums over the cartesian coordinates x, y, z and Ω is the unit cell volume. In a very similar way we can derive expressions for the non-local contribution to the force on the ions within the Kleinman–Bylander scheme. As for the local component of the force the Hellmann–Feynman theorem is used (e.g. Srivastava and Weaire 1987). As an example, the $l = 1$ contribution becomes

$$\boldsymbol{F}_\mu^{\mathrm{NL}} = \frac{24\pi}{\Omega I^{\mathrm{s}}_{\mu,1}} \operatorname{Im} \sum_{i,n,k} \left(\sum_{\boldsymbol{g}} g\, c_{n,\boldsymbol{g}} \frac{(\boldsymbol{k}+\boldsymbol{g})_i}{k+g} \exp(-\mathrm{i}\boldsymbol{g}\cdot\boldsymbol{r}_\mu)\, I_{\mu,1}(k+g) \right.$$
$$\left. \times \sum_{\boldsymbol{g}'} c_{n,\boldsymbol{g}'} \frac{(\boldsymbol{k}+\boldsymbol{g}')_i}{k+g'} \exp(\mathrm{i}\boldsymbol{g}'\cdot\boldsymbol{r}_\mu)\, I_{\mu,1}(k+g') \right) \tag{8}$$

where Im represents the imaginary part. The $l = 0$ and $l = 2$ force components have a very similar form which may be derived by comparison of (8) and (7*b*). The separation (4) of the pseudopotential means that the number of operations required to evaluate (7) and (8) now scales as N because the sums over $\boldsymbol{g}'$ need be performed only once at each timestep. However, a fairly large number of operations may still be required; in the $l = 2$ contribution of (7c), *nine* $\boldsymbol{g}'$ sums are needed for the (i, j) components. The non-local electron and ion dynamics can now be encoded straightforwardly and this simply adds two subroutines to existing Car–Parrinello programs.

A number of tests have been carried out, to check both the coding of the non-local potential contributions and whether the hitherto little used Kleinman and Bylander (1982) potentials give results that are as good as conventional, non-separable schemes. Silicon, in various forms, has been used as the test material. Norm-conserving pseudopotentials were generated using the method described by Kerker (1980), with silicon in a $3s^2 3p^1 3d^{0.5}$ configuration. The Ceperley–Alder exchange-correlation functional was used, as parametrized by Perdew and Zunger (1981). The form of the projection integrals (5a) for various choices of local potential are shown in figure 1. In order to compare the local and non-local contributions we plot both $V^{\mathrm{L}}(q)$ and its most obvious non-local equivalent, $4\pi I_0(0) I_0(q)/I_0^{\mathrm{s}}$ (see (4)). Although only the $l = 0$ correction can be visualized in this way, it does show the relative sizes of the local and non-local potentials and their respective q dependences.

The coding of the non-local electronic forces (7) was tested first by calculating the electronic structure of a 'crystal' containing one silicon atom per simple cubic unit cell, with a lattice parameter of 10 Å. Clearly, the results should be very similar to those obtained for an isolated atom. We used a Fourier transform box with $(24)^3$ points and a kinetic energy cut-off of 11.0 Ryd, which generates 4139 plane waves. A single k-point at (0,0,0) was used. Despite the large number of plane waves the calculation converges quickly—convergence of the total energy to one part in 10^5 was obtained after about fifty molecular dynamics timesteps. Results for the total energy and the lowest two eigenvalues are shown in table 1. It can be seen that whether the $l = 0, 1$ or 2 component is taken to be the local pseudopotential, the non-local corrections return the total energy and eigenvalues to very similar values. The eigenvalues should also be compared with those for a neutral silicon atom; 3s = −0.80 Ryd, 3p = −0.31 Ryd.

The non-local contributions to the Hellmann–Feynman forces (8) were tested with two silicon atoms in the same cubic cell. With their separations differing by 5×10^{-4} Å

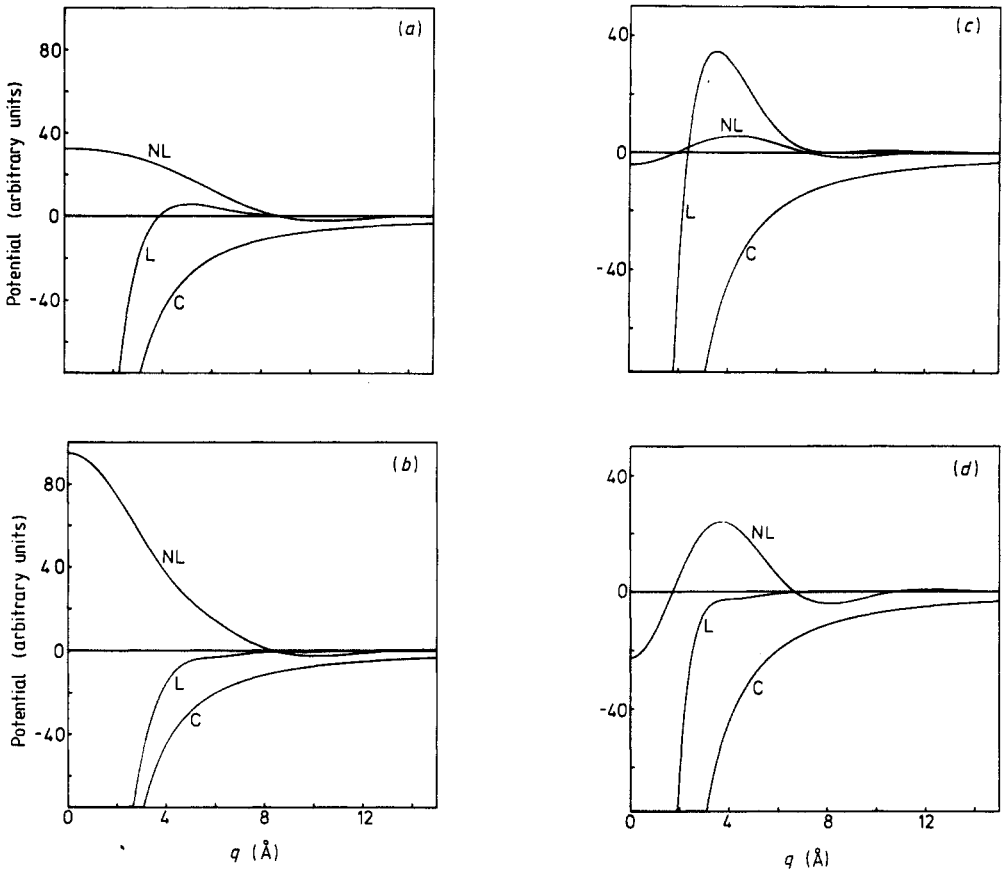

Figure 1. Comparison of local and non-local potentials in k-space. In all cases curve L is the local part $V^{L}(q)$ and curve NL is the non-local contribution $4\pi I_0(0)I_0(q)/I_0^s$. For comparison the Fourier transform of the ionic Coulomb potential is also shown (curve C). The vertical scale is arbitrary but consistent between figures. The horizontal scale is q in Å^{-1}. (*a*) Si, $l = 1$ local; (*b*) Si, $l = 2$ local; (*c*) Sn, $l = 1$ local; (*d*) Sn, $l = 2$ local.

Table 1. Comparison of the total energy and eigenvalues from local (bracketed) and non-local calculations of a single Si atom in a 10 Å cubic cell, for various choices of the local potential.

Local component	$l = 0$	$l = 1$	$l = 2$
Total energy (Ryd)	−7.41 (−7.31)	−7.42 (−8.04)	−7.42 (−11.06)
3s eigenvalue (Ryd)	−0.78 (−0.82)	−0.78 (−1.00)	−0.77 (−1.71)
3p eigenvalue (Ryd)	−0.27 (−0.25)	−0.26 (−0.22)	−0.26 (−0.23)

the electronic system was relaxed to the ground state and the ion forces compared with values obtained numerically from total energy differences. Again, excellent agreement was obtained. Our final tests involved eight silicon atoms in a cubic cell. For these calculations a cut-off of 7.35 Ryd was used, which corresponds to using about 450 plane waves. The lattice parameter was varied between 5 Å and 6 Å, and the Fourier transform box had $(16)^3$ points. Runs were performed both with the ions starting

in their correct positions within the diamond structure and with displaced starting positions. Electronic convergence took about 300 timesteps, and in calculations where the ions were displaced, a further 200 steps were necessary for them to settle into the diamond structure, with residual forces of less than 0.01 eV $Å^{-1}$. After this number of steps the total energy had converged to about one part in 10^6. With a single $\boldsymbol{k}$-point at $(\frac{1}{4},\frac{1}{4},\frac{1}{4})$ we found a minimum total energy of 7.87 Ryd per atom at a lattice parameter of 5.39 Å. This agrees well with other more conventional pseudopotential calculations (e.g. Yin and Cohen 1982).

The amount of extra computing that is introduced by the non-local corrections depends very much on the problem in hand. If there are N plane waves, M occupied bands and P atoms in the unit cell, both (7) and (8) involve $\sim N \times M \times P$ terms. The local contributions scale differently because of the repeated use of FFTs. To give some examples: for the eight atom calculations referred to above the time spent in the non-local subroutines varied from 75% of the total time for a calculation where the $l = 0$ pseudopotential is taken to be local to 47% for $l = 2$ local. This difference simply reflects the different number of components (i, j) which appear in (7*a*), (7*b*) and (7*c*). For the one atom per cell calculations the non-local contributions form a much smaller proportion of the total time; as little as 17% for the $l = 2$ local calculation. In general, it can be seen that the inclusion of non-local pseudopotentials does increase the computational requirements of the Car–Parrinello method, but not to the extent that calculations become severely limited.

3. Adsorbate-induced surface reconstruction

The reconstruction of the Si(111) surface due to adsorbed atoms has recently attracted considerable attention, both theoretically and experimentally (e.g. Northrup 1984, Nicholls *et al* 1987, Hamers and Demuth 1988, Bedrossian *et al* 1989, Lyo *et al* 1989). Our interest stems from a recent x-ray diffraction study of the Si(111) $\sqrt{3} \times \sqrt{3}$–Sn reconstructed surface (Conway *et al* 1989). The experimentally determined structure is shown schematically in figure 2 and the structural parameters are listed in table 2. In this paper we use this system basically as a test of our non-local Car–Parrinello code; more details of the electronic structure will be presented elsewhere (Ramchurn *et al* 1990). In particular, we look at the H_3 and T_4 adsorbate sites (Northrup 1984), comparing their total energies and analysing the surface and sub-surface reconstruction.

Table 2. Structural parameters for the T_4 reconstruction (see figure 2). The Δ represent vertical displacements (+ is up, − is down) and the a represent lateral displacements (− is towards Sn atoms, + is away). For our theoretical results we estimate errors of about ±0.03 Å.

Displacement	Theory (Å)	Experiment (Å)
$\Delta 2$	+0.29	+0.20
$\Delta 2'$	−0.48	−0.42
$\Delta 3$	+0.07	+0.17
$\Delta 3'$	−0.15	−0.35
a_1	−0.13	−0.21
a_4	+0.05	+0.10

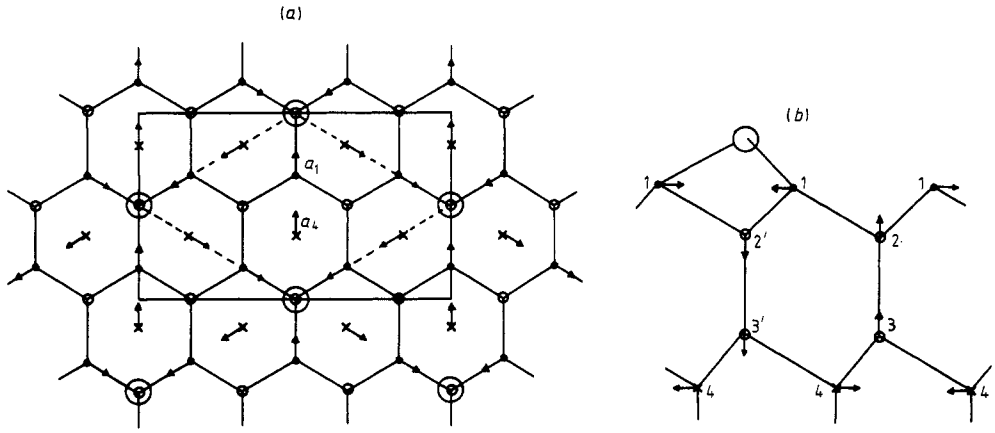

Figure 2. (*a*) Plan view of the T_4 chemisorption site showing both $\sqrt{3} \times \sqrt{3}$ (dotted) and orthorhombic cells. Top layer silicon atoms (full circles), second and third layers (small open circles), and fourth and fifth layers (crosses) are also shown. Large open circles represent the Sn adatoms. Arrows (not to scale) represent directions of displacements in the relaxed structure. In the H_3 site the adatoms sit above fourth and fifth layer atoms. (*b*) Side view of the T_4 structure. The notation is the same as in (*a*).

In our calculations periodicity normal to the surface is obtained using a supercell which consists of four double layers of silicon separated by 2.4 double layers of vacuum. Tin atoms are placed on both top and bottom surfaces. This means that our subsurface reconstruction can only be expected to be reliable in the first double layer. The second double layers in from the top and bottom surfaces must interact to some extent and, of course, no information can be recovered about the third and deeper double layers. The Sn pseudopotentials were generated with a $5s^2 5p^1 5d^{0.5}$ reference configuration and were subjected to the same tests as described for Si above. The form of the projection integrals (5) is shown in figure 1. For both Si and Sn the $l = 1$ component of the pseudopotential was chosen to be the local part.

In order to keep the total energy minimization as unbiased as possible we have used an orthorhombic unit cell instead of the hexagonal cell of the $\sqrt{3} \times \sqrt{3}$ structure (figure 2). This enables us to determine whether the $\sqrt{3} \times \sqrt{3}$ cell is stable relative to an uncentred $3 \times \sqrt{3}$ reconstruction. Similarly, we do not impose the $3m$ point symmetry which is assumed in the experimental determination. Thus *any* structure within the orthorhombic cell could in principle be found. However, because of the size of the calculation a smaller kinetic energy cut-off (5.88 Ryd) than that used previously is used here. The theoretical lattice constant for Si at this cut-off is found to be 5.44 Å, which gives lattice parameters for the orthorhombic supercell of $a = 11.54$ Å, $b = 6.66$ Å, $c = 17.66$ Å. A single $\boldsymbol{k}$-point at (0,0,0) is used, yielding a 2213 plane wave calculation. The Fourier transform box has dimensions $27 \times 16 \times 36$. With 52 atoms in the unit cell, the energy functional therefore has to be minimized with respect to (104×2213) complex variational parameters. Electronic convergence now requires about 400 timesteps while overall convergence of the atomic structure is obtained by the 700th timestep. Although these calculations are probably too small, both in the $\boldsymbol{k}$-point density and the kinetic energy cut-off, to produce highly accurate total energies and atomic positions, the work of Meade and Vanderbilt (1989) on related systems indicates that smaller calculations do find the same basic structure as very large ones.

Our calculations have been performed on a SUN4 workstation, the longest runs taking about 300 h. With greater computational resources the results could clearly be refined.

Relaxation of the structure was performed with the Sn atoms starting in both H_3 (above fourth single layer atoms) and T_4 (above second layer atoms) sites. As found by Northrup (1984) in his calculations on Al adsorption on Si(111), if the substrate is not allowed to relax we find the H_3 site to be energetically favourable. However, when unconstrained relaxation is allowed the final T_4 structure is found to be more stable than the H_3 by 0.3 eV per adatom, again in line with Northrup's (1984) calculations. The minimum energy structure *is* found to adopt a $\sqrt{3} \times \sqrt{3}$ cell and to retain $3m$ symmetry to a high degree of accuracy. The maximum difference in the positions of any two atoms which are related by the $3m$ symmetry of the x-ray determined structure is 0.03 Å, which should be compared to the maximum displacements of about 0.4 Å. Similarly, inversion symmetry about the centre of the slab is retained to a high accuracy.

Top and side views of the T_4 relaxed structure are shown in figures 2(a) and 2(b) respectively. Numerical values of the displacements are given in table 2, where our theoretical values are compared with the experimental data of Conway *et al* (1989). The agreement is seen to be very good, both in the sign and the magnitude of the displacements. The greatest discrepancy occurs for the third and fourth layer displacements which, as discussed above, is not surprising given our slab geometry. We find the Sn atoms to sit 1.44 ± 0.05 Å above the surface, compared with experimental values of 1.44 ± 0.32 Å or 1.59 Å, depending on the type of fit that was used.

In conclusion, we have shown that our implementation of a non-local Car–Parrinello code is capable of performing large-scale total energy minimization. We are happy to provide the programs to interested researchers—contact should be made via electronic mail to pysdb@uk.ac.bath.gdr.

Acknowledgments

We wish to thank M C Payne for providing us with the original local Car–Parrinello code and for helpful discussions. This work is supported by the Science and Engineering Research Council.

References

Allan D C and Teter M P 1987 *Phys. Rev. Lett.* **59** 1136
Ballone P, Andreoni W, Car R and Parrinello M 1988 *Phys. Rev. Lett.* **60** 271
Bedrossian P *et al* 1989 *Phys. Rev. Lett.* **63** 1257
Car R and Parrinello M 1985 *Phys. Rev. Lett.* **55** 2471
Conway K M, Macdonald J E, Norris C, Vlieg E and van der Veen J F 1989 *Surf. Sci.* **215** 555
Hamers R J and Demuth J E 1988 *Phys. Rev. Lett.* **60** 2527
Ihm J 1988 *Rep. Prog. Phys.* **51** 105
Lyo I W, Kaxiras E and Avouris P 1989 *Phys. Rev. Lett.* **63** 1261
Kerker G P 1980 *J. Phys. C: Solid State Phys.* **13** L189
Kleinman L and Bylander D M 1982 *Phys. Rev. Lett.* **48** 1425
Kohn W and Sham L J 1965 *Phys. Rev.* **140** A1133
Meade R D and Vanderbilt D 1989 *Phys. Rev.* B **40** 3905
Needels M, Payne M C and Joannopoulos J D 1987 *Phys. Rev. Lett.* **58** 1765
Nex C M M 1987 *J. Comp. Phys.* **70** 138
Nicholls J M, Reihl B and Northrup J E 1987 *Phys. Rev.* B **35** 4137

Northrup J E 1984 *Phys. Rev. Lett.* **53** 683
Payne M C 1987 *J. Phys. C: Solid State Phys.* **20** L983
Payne M C, Allan D C, Teter M P and Joannopoulos J D 1990 *Rev. Mod. Phys.* to be published
Payne M C, Bristowe P D and Joannopoulos J D 1987 *Phys. Rev. Lett.* **58** 1348
Payne M C, Joannopoulos J D, Allan D C, Teter M P and Vanderbilt D H 1986 *Phys. Rev. Lett.* **56** 2656
Perdew J P and Zunger A 1981 *Phys. Rev.* B **23** 5048
Ramchurn S K, Bird D M and Bullett D W 1990 to be published
Srivastava G P and Weaire D 1987 *Adv. Phys.* **36** 463
Yin M T and Cohen M L 1982 *Phys. Rev.* B **26** 5668